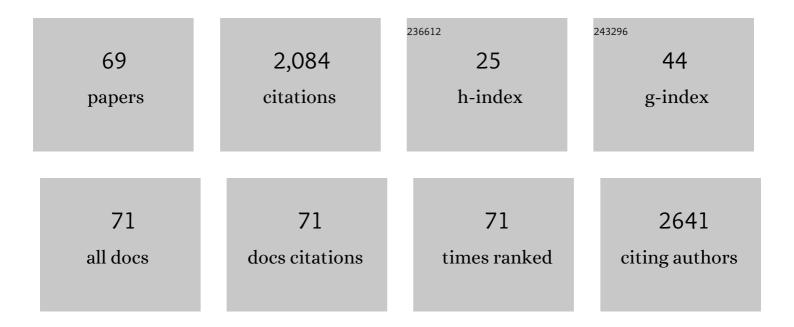
List of Publications by Year in descending order

Source: https://exaly.com/author-pdf/1208761/publications.pdf Version: 2024-02-01



YAN KONC

#	Article	IF	CITATIONS
1	A Facile Oneâ€Step Synthesis of Feâ€Doped gâ€C ₃ N ₄ Nanosheets and Their Improved Visibleâ€Light Photocatalytic Performance. ChemCatChem, 2017, 9, 1708-1715.	1.8	278
2	A Metalâ€Free Donor–Acceptor Covalent Organic Framework Photocatalyst for Visibleâ€Lightâ€Driven Reduction of CO ₂ with H ₂ O. ChemSusChem, 2020, 13, 1725-1729.	3.6	177
3	Construction of 3D hierarchical microarchitectures of Z-scheme UiO-66-(COOH)2/ZnIn2S4 hybrid decorated with non-noble MoS2 cocatalyst: A highly efficient photocatalyst for hydrogen evolution and Cr(VI) reduction. Chemical Engineering Journal, 2020, 384, 123352.	6.6	137
4	Engineering carbon-defects on ultrathin g-C3N4 allows one-pot output and dramatically boosts photoredox catalytic activity. Applied Catalysis B: Environmental, 2021, 295, 120272.	10.8	129
5	Silver-Incorporated Mussel-Inspired Polydopamine Coatings on Mesoporous Silica as an Efficient Nanocatalyst and Antimicrobial Agent. ACS Applied Materials & Interfaces, 2018, 10, 1792-1801.	4.0	116
6	The states of vanadium species in V-SBA-15 synthesized under different pH values. Microporous and Mesoporous Materials, 2008, 110, 508-516.	2.2	79
7	Synthesis, characterization and catalytic performance for phenol hydroxylation of Fe-MCM41 with high iron content. Microporous and Mesoporous Materials, 2008, 113, 163-170.	2.2	77
8	Improved visible light photocatalytic activity of fluorine and nitrogen co-doped TiO2 with tunable nanoparticle size. Applied Surface Science, 2015, 332, 573-580.	3.1	57
9	Synthesis, characterization of bimetallic Ce–Fe-SBA-15 and its catalytic performance in the phenol hydroxylation. Microporous and Mesoporous Materials, 2008, 113, 393-401.	2.2	50
10	Defects remodeling of g-C3N4 nanosheets by fluorine-containing solvothermal treatment to enhance their photocatalytic activities. Applied Surface Science, 2019, 474, 194-202.	3.1	42
11	In situ embedding of ultra-fine nickel oxide nanoparticles in HMS with enhanced catalytic activities of styrene epoxidation. Microporous and Mesoporous Materials, 2017, 238, 69-77.	2.2	39
12	Construction of a novel Ag/Ag3PO4/MIL-68(In)-NH2 plasmonic heterojunction photocatalyst for high-efficiency photocatalysis. Journal of Materials Science and Technology, 2022, 101, 37-48.	5.6	39
13	Metal-organic framework-derived rodlike AgCl/Ag/In2O3: A plasmonic Z-scheme visible light photocatalyst. Chemical Engineering Journal, 2021, 415, 129010.	6.6	38
14	Synthesis and characterization of Cu–Ti–MCM41. Microporous and Mesoporous Materials, 2005, 86, 191-197.	2.2	35
15	Oriented surface decoration of (Co-Mn) bimetal oxides on nanospherical porous silica and synergetic effect in biomass-derived 5-hydroxymethylfurfural oxidation. Molecular Catalysis, 2017, 435, 144-155.	1.0	34
16	Coordination of manganese porphyrins on amino-functionalized MCM-41 for heterogeneous catalysis of naphthalene hydroxylation. Chinese Journal of Catalysis, 2015, 36, 1035-1041.	6.9	32
17	Synthesis, characterization and catalytic activity of binary metallic titanium and iron containing mesoporous silica. Microporous and Mesoporous Materials, 2012, 162, 51-59.	2.2	31
18	Nanosheet-like Ni-based metasilicate towards the regulated catalytic activity in styrene oxidation via introducing heteroatom metal. Applied Surface Science, 2019, 471, 822-834.	3.1	30

#	Article	lF	CITATIONS
19	Photocatalytic producing dihydroxybenzenes from phenol enabled by gathering oxygen vacancies in ultrathin porous ZnO nanosheets. Applied Surface Science, 2020, 505, 144580.	3.1	30
20	The Complete Control for the Nanosize of Spherical MCM-41. Journal of Nanoscience and Nanotechnology, 2012, 12, 7239-7249.	0.9	28
21	Spherical V-MCM-48: the synthesis, characterization and catalytic performance in styrene oxidation. RSC Advances, 2014, 4, 50832-50839.	1.7	27
22	Degradation of phenol in industrial wastewater over the F–Fe/TiO2 photocatalysts under visible light illumination. Chinese Journal of Chemical Engineering, 2016, 24, 1712-1718.	1.7	27
23	Engineering 2D compressed layered g-C3N4 nanosheets by the intercalation of BiVO4-Bi2WO6 composites for boosting photocatalytic activities. Applied Surface Science, 2021, 557, 149796.	3.1	27
24	Micropore-enriched CuO-based silica catalyst directly prepared by anionic template-induced method and its boosting catalytic activity in olefins epoxidation. Microporous and Mesoporous Materials, 2017, 246, 215-224.	2.2	26
25	In situ incorporation of well-dispersed Cu–Fe oxides in the mesochannels of AMS and their utilization as catalysts towards the Fenton-like degradation of methylene blue. Journal of Materials Science, 2017, 52, 1432-1445.	1.7	25
26	Spherical V-Fe-MCM-48: The Synthesis, Characterization and Hydrothermal Stability. Materials, 2015, 8, 1752-1765.	1.3	24
27	Direct templating assembly route for the preparation of highly-dispersed vanadia species encapsulated in mesoporous MCM-41 channel. RSC Advances, 2015, 5, 72099-72106.	1.7	23
28	A metal-assisted templating route (S ^O M ⁺ I ^{â^'}) for fabricating thin-layer CoO covered on the channel of nanospherical-HMS with improved catalytic properties. Dalton Transactions, 2016, 45, 6371-6382.	1.6	21
29	<i>In situ</i> intercalation of Au nanoparticles and magnetic γ-Fe ₂ O ₃ in the walls of MCM-41 with abundant void defects for highly efficient reduction of 4-nitrophenol and organic dyes. Dalton Transactions, 2018, 47, 16862-16875.	1.6	20
30	Bimetallic metal–organic frameworks-derived mesoporous CdxZn1â~`xS polyhedrons for enhanced photocatalytic hydrogen evolution. Journal of Materials Research, 2019, 34, 1773-1784.	1.2	20
31	Beltâ€Like Cobalt Phosphate Tetrahydrate as the Nonâ€Noble Metal Catalyst with Enhanced Catalytic Reduction Activity. ChemistrySelect, 2018, 3, 6924-6934.	0.7	19
32	Neighboring Cu toward Mn site in confined mesopore to trigger strong interplay for boosting catalytic epoxidation of styrene. Applied Surface Science, 2021, 537, 148100.	3.1	19
33	Thermal-induced surface defective Co/Fe–Co planar hybrid composite nanosheet with enhanced catalytic activity in the Fenton-like reaction. Materials Chemistry Frontiers, 2017, 1, 2065-2077.	3.2	17
34	Enabling synchronous activation of inner-core and mesoporous outer-shell of monodispersed Fe3O4@SiO2 by in-situ implanted MnO to synergistically deliver enhanced catalytic activity. Journal of Alloys and Compounds, 2020, 842, 155817.	2.8	17
35	Synthesis, characterization of bimetallic Sn-Zn-MCM41 and its catalytic performance in the hydroxylation of phenol. Journal of Porous Materials, 2006, 13, 341-346.	1.3	16
36	Effect of Promoters on the Catalytic Activity of MCM-41 with High Copper Content in Benzene Hydroxylation. Chinese Journal of Catalysis, 2008, 29, 385-390.	6.9	16

#	Article	IF	CITATIONS
37	An iron-based micropore-enriched silica catalyst: in situ confining of Fe ₂ O ₃ in the mesopores and its improved catalytic properties. RSC Advances, 2016, 6, 76064-76074.	1.7	15
38	High promoting of selective oxidation of ethylbenzene by Mn-ZSM-5 synthesized without organic template and calcination. Research on Chemical Intermediates, 2020, 46, 2817-2832.	1.3	15
39	Preparation of ZSM-5 containing vanadium and BrĄ̃nsted acid sites with high promoting of styrene oxidation using 30% H2O2. Chinese Journal of Chemical Engineering, 2020, 28, 1302-1310.	1.7	15
40	Oneâ€Pot Synthesis of Iron ontaining Nanoreactors with Controllable Catalytic Activity Based on Multichannel Mesoporous Silica. ChemCatChem, 2015, 7, 3855-3864.	1.8	14
41	Effects of synergetic effect between Co and γ-Fe2O3 in confined silica matrix of MCM-41 on the formation of free radicals for the advanced oxidation technology. Applied Surface Science, 2020, 527, 146853.	3.1	14
42	Acid-redox bifunctional Fe/Al-AMS catalyst: Simultaneously oriented introducing Fe2O3 in the channels and Al in the framework of AMS and its enhanced catalytic performance. Applied Catalysis A: General, 2019, 575, 159-169.	2.2	13
43	Facilely self-reduced generation of Ag nanowires in the confined reductive siliceous nanopores and its catalytic reduction property. Journal of Alloys and Compounds, 2017, 719, 30-41.	2.8	12
44	Engineering Z-system hybrids of 0D/2D F-TiO ₂ quantum dots/g-C ₃ N ₄ heterostructures through chemical bonds with enhanced visible-light photocatalytic performance. New Journal of Chemistry, 2021, 45, 3067-3078.	1.4	12
45	Synthesis of ordered hexagonal porous tin-doped zirconium oxides with a high surface area. Microporous and Mesoporous Materials, 2005, 77, 241-243.	2.2	11
46	Improvement on the mesostructural ordering and catalytic activity of Co-MCM-41 with ascorbic acid as auxiliary. Materials Letters, 2013, 100, 159-162.	1.3	11
47	Raspberry-Like Bismuth Oxychloride on Mesoporous Siliceous Support for Sensitive Electrochemical Stripping Analysis of Cadmium. Molecules, 2017, 22, 797.	1.7	9
48	Stabilized Pony‣izedâ€CuFe ₂ O ₄ /Carbon Nitride Porous Composites with Boosting Fentonâ€like Oxidation Activity. ChemistrySelect, 2018, 3, 4207-4216.	0.7	9
49	Oriented Decoration in Metal-Functionalized Ordered Mesoporous Silicas and Their Catalytic Applications in the Oxidation of Aromatic Compounds. Catalysts, 2018, 8, 80.	1.6	9
50	Density Functional Theory Study of Small Au Nanoparticles Anchored on the Inner Surface of Mesoporous Co ₃ O ₄ for the Catalytic Reduction of 4-Nitrophenol. ACS Applied Nano Materials, 2021, 4, 4763-4773.	2.4	9
51	Aminosilane decorated carbon template-induced in situ encapsulation of multiple-Ag-cores inside mesoporous hollow silica. RSC Advances, 2016, 6, 30852-30861.	1.7	8
52	Exposed ternary metal active sites on mesoporous channels: A promising catalyst for low-temperature selective catalytic oxidization of phenol with H2O2. Molecular Catalysis, 2019, 478, 110568.	1.0	8
53	Template-induced in situ dispersion of enhanced basic-sites on sponge-like mesoporous silica and its improved catalytic property. RSC Advances, 2016, 6, 91968-91980.	1.7	7
54	The structure-property relationship of oxovanadium(IV) complexes in the wall framework of PMOs and their catalytic applications. Applied Surface Science, 2017, 397, 183-191.	3.1	7

#	Article	IF	CITATIONS
55	Self-assembly of the chaperonin GroEL nanocage induced at submicellar detergent. Scientific Reports, 2014, 4, 5614.	1.6	6
56	Regeneration of Arrayed Gold Microelectrodes Equipped for a Real-Time Cell Analyzer. Journal of Visualized Experiments, 2018, , .	0.2	6
57	Enriched Ag Nanospecies Interspersed Nanoporous Siliceous Antibacterial Agent. ChemistrySelect, 2018, 3, 10255-10258.	0.7	6
58	Synergy Derived from Bimetal Coâ^'Cu in Phosphate to Enables Ultrafast Catalytic Hydrogenated Activity in Nitrophenol Reduction. ChemistrySelect, 2020, 5, 3405-3412.	0.7	6
59	Record-high catalytic hydrogenated activity in nitroarenes reduction derived from in-situ nascent active metals enabled by constructing bimetallic phosphate. Molecular Catalysis, 2020, 486, 110873.	1.0	6
60	Synthesis and Characterization of Novel Super Microporous Tin-doped Zirconium Oxide. Chinese Journal of Chemistry, 2005, 23, 1584-1588.	2.6	5
61	Templateâ€Free Synthesis of Highâ€Content Vanadiumâ€Doped ZSMâ€5 with Enhanced Catalytic Performance. ChemistrySelect, 2017, 2, 11513-11520.	0.7	5
62	Probing the formation and optical properties of Ti3+–TiO2 with (001) exposed crystal facet by ethanol-assisted fluorination. New Journal of Chemistry, 2021, 45, 12453-12463.	1.4	5
63	Synthesis of F-TiO ₂ Nanosheets and its Photocatalytic Oxidation of Benzene to Phenol. Advanced Materials Research, 2013, 750-752, 1160-1163.	0.3	4
64	Threeâ€Dimensionally Controllable Synthesis of Multichannel Silica Nanotubes and Their Application as Dual Drug Carriers. ChemPlusChem, 2015, 80, 1615-1623.	1.3	3
65	A Facile Method for the Direct Introduction of FeO _x in Mesoporous AMS Through A Templating Route (S ^{â^'} [MN] ⁺ l ^{â^'}) and Its Catalytic Application. ChemistrySelect, 2016, 1, 1305-1313.	0.7	3
66	Mesopore-encaged V-Mn oxides: Progressive insertion approach triggering reconstructed active sites to enhance catalytic oxidative desulfuration. Chinese Journal of Chemical Engineering, 2022, 45, 182-193.	1.7	3
67	Influences of Pore Sizes on the Catalytic Activity of Fe-MCM-41 in Hydroxylation of Phenol. Asian Journal of Chemistry, 2013, 25, 9087-9091.	0.1	2
68	Synthesis, Characterization and Catalytic Activity of Nano-Spherical MCM-41 Modified with Vanadium. Journal of Nanoscience and Nanotechnology, 2014, 14, 7300-7306.	0.9	2
69	Micro-morphology highly uniform mesoporous Co3O4 spheres: shape-controlled fabrication by a salt-assisted template-free method and enhanced catalytic performance of styrene epoxidation. Journal of Materials Science, 2022, 57, 11546-11562.	1.7	1